**Response to Referee 1**

COMMENT 1. Page 1 line 1: I suggest specifying the (geographic) scale where the model can be applied and also the scale of the "regions". line 2: Splitting "horizontally" is ambiguous. It can be understood as splitting with horizontal planes. I suggest using e.g. "split in the horizontal plane". line 7: I suggest adding some quantitative results, e.g. the number 0.05 mentioned in Conclusions.

REPLY 1. The first line now says "vegetation canopies" rather than "vegetation" to make clear that radiation is treated at a larger scale than individual trees. The final sentence talks about weather and climate modelling, so the scale is then clearly the size of a gridbox of such models. The phrase "split in the horizontal plane" is now used, and the root-mean-squared differences in reflectance, transmittance and canopy absorptance have now been stated.

COMMENT 2. Page 2: The description of clumping is misleading. Clumping is also used to describe vegetation structure variation in the vertical direction and at scales smaller than a tree crown. This should be mentioned as the current description can be misleading with respect to the universality of the proposed approach.

REPLY 2. The text has been changed accordingly.

COMMENT 3. Page 3 line 4: add "constant thickness" after "canopy layer". I see no need for quatition marks.

REPLY 3. "Constant thickness" has been added. The quotation marks are to clarify that "canopy layer" and "sub-canopy layer" are named layers in the formulation of the problem, as shown in Fig. 1.

COMMENT 4. ...line 4: Define what is meant by "domain" line 4: Again, choose an anambigous term instead of "divided horizontally" (although the meaning can be inferred from context). line 4: The concept of "region" should be defined here and not on the following page. It is counterintuitive to have a region consisting of separate parts.

REPLY 4. I've expanded to "horizontal domain (corresponding to a weather- or climate-model gridbox)". The definition of region has been improved. In no case in this paper does a region consist of separate parts. But a tree can be represented by separate regions (as shown in Fig. 1).

COMMENT 5. ...line 4: The necessity of up to two vegetated regions is not justified and not followed later in the manuscript.

REPLY 5. The need for two vegetated regions is justified in Fig. 6 of the original manuscript: when only one vegetated region is used, a worse result is obtained. In the new manuscript, the results for one vegetated region are added to Figs. 2-5. Section 2.1 now makes reference to these results in section 3.

COMMENT 6. ...line 7: How would the situation of objects not being cylinders (highly grouped canopies) affect accuracy? In my opinion, this is explicitly assumed here. Although not mathematically, but the results are only provided for canopies with clearly separable crowns.

REPLY 6. The new text at the end of section 2.3 explains how the assumptions in SPARTACUS are only that the vegetation is randomly separated, not that it is composed of cylindrical crowns. However, it will need to wait until a future paper to test this since we only have Monte Carlo results from RAMI4PILPS where the nature of the canopy is rather geometrically simple.

COMMENT 7. ...line 8: Define "vegetation element". E.g., is it a leaf or a tree crown? line 9: Unclear what is meant by "same": a canopy layer is first and foremost defined by leaf area density. line 10: Why possible omission is only mentioned for shrubland?

REPLY 7. These terms have been clarified: "vegetation element" replaced by "tree crown", and the phrase containing "same" replaced with "also divided into m regions (see Fig. 1)". The mention of shrubland has been removed.

COMMENT 8. Page 4 line 1: Define what a,b,c stand for (different regions). Probably, it needs to be done earlier as line 13 of previous page already refers to L^ab. In hindsight, it is clear that a and b refer to two regions.

REPLY 8. Now defined in section 2.1.

COMMENT 9. ...line 1: In optical radiometry, radiant power is the same as radiant flux. Use only one of these terms consistently. FLux per surface area (flux density) is irradiance. "Domain-mean" flux is a contradictory term. Irradiance can be averaged, but flux being total power can only be added. The correct term would be domain-total flux, the sum all flux components over the domain. (note: in many other fields, flux is power divided by area)

REPLY 9. All uses of flux where such an ambiguity can arise have been replaced by irradiance.

COMMENT 10. ...line 3: This line contains the definition of a "region". It should be given earlier.

REPLY 10. It is now given in section 2.1.

COMMENT 11. Page 5 line 25: rewrite as LAI/(2 Delta z)

REPLY 11. Done.

COMMENT 12. line 32: citation needed for the equations.

REPLY 12. Citation provided (Pinty et al. 2006).

COMMENT 13. Page 6 line 8: Give some justifications for this rather arbitrary assumption and also discuss its consequences.

REPLY 13. The justification is that it was found by Shonk and Hogan (2008) to be the best assumption for representing the PDF of cloud optical depth, as is stated. Further justification is provided by the good a-posteriori agreement with Monte Carlo, shown in the results section.

COMMENT 14. line 12: Unclear what is meant by "random" and why it's necessary. Different random processes can dreate very different tree distribution patterns, but very few create non-overlapping crowns. Instead of "random", why cannot the trees in the "idealized forest" be situated on a regular grid?

REPLY 14. We have now explaned mathematically at the end of section 2.3 how the SPARTACUS formulation implies a random distribution of trees. Specifically, it assumes that the chord lengths between the edges of tree crowns in all possible horizontal directions follow an exponential distribution. If the trees were on a regular grid, their spacing distribution would be far from exponential, and the assumption would be violated.

COMMENT 15. Page 11 line 4: Choose either PAR or "visible region"; alternatively, add "and" between the two.

REPLY 15. We believe that the text reads better if it is kept the same: the spectral interval from 400 to 700 nm is both photosynthetically active and the range detectable by the human eye. Adding an "and" would make the phrase more confusing when it is immediately followed by "and the near-infrared".

COMMENT 16. ...line 7: Be moerelaborate on the approximation method.

REPLY 16. The explanatory text that follows has been expanded - see also the reply to Referee 2's Comment 3.

COMMENT 17. ...line 7: A sphere (or, a single tree crown) does have a LAI value. LAI is only defined for a region which usually includes betweem-element gaps, e.g., a forest stand. It can indeed be defined for the area of a single crown, but this contradicts the common practice. line 8: Clarify what is meant by "upper" and "lower". These do not seem to refer to canopy location (but can be understood to).

REPLY 17. Where possible, such discussion is rephrased in terms of zenith optical depth. However, Widlowski et al. (2011) did use LAI in this context in their Table 1, so we do too in our Table 1 but with more explanation. "Upper" and "lower" refer to parts of the zenith optical depth distribution, not vertical location. We have tried to make this clearer.

COMMENT 18. Page 12 line 2: Again, "domain-main flux" needs clarification. line 11: Again, I suggest avoiding the use of LAI for a single tree. It is straightforward for ideal cylindrical tree crowns, but can cause much confusion when attempted in a natural situation where tree crowns do not have a clearly distinguishable bounding surface.

REPLY 17. Rephrased.

COMMENT 18. Page 14 The section "Conclusions" contains mostly discussion and should be renamed. No new issues should be brought up in Conclusions and citations are unnecessary. Instead, the statements should be based on what was presented earlier, mainly Discussion – a section clearly missing from the manuscript. The current Conclusions contains many new topics and even a value (0.05 on line 11, which should be mentioned in the results section).

REPLY 18. Root-mean-squared errors are now computed and stated in the results section. The final section has been renamed "Discussion and conclusions"

**Response to Referee 2**

COMMENT 1. Page 3, line 7. Please add “ly" after “explicit."

REPLY 1. Done

COMMENT 2. Page 6, lines 10–21. I am unclear about the fundamental parameter here. The equations require L^ab. Is this what you would measure in the field, or would you measure D and infer L^ab? In the former case, D is just an illustrative diameter, but is more fundamental in the latter case. In the case of dense canopies, if L^ab is measured, what is the purpose of S, the meaning of which is unclear? Conversely, if you infer L^ab from S, how is S determined in the field?

REPLY 2. The fundamental parameter for 3D radiation is L^ab. However, this depends on both the areal coverage of trees "c_v", and the properties of an individual representative tree. In the context of a weather or climate simulation, we would use a global dataset of c_v (e.g. from Hansen et al) but would need to estimate L^ab from it. This can be done by introducing an additional parameter representing the size of an individual tree, and the manuscript describes two models for how this could be done (D and S); to be useful, the parameter used would need to be independent of c_v. To compute D and S in the field, we would measure L^ab and c_v and apply inverted forms of equations 17 and 18. D is needed for comparison with the Monte Carlo results in the present manuscript which assumed tree crowns not to touch. The manuscript has been extended to clarify all these points in new section 2.4.

COMMENT 3. Page 11, lines 6–9. I assume that regions b and c still have the same area, as noted on page 6. It would be useful to remind the reader of this. On line 8, the argument should apply to any sphere, not just one with an LAI of 5. It is not clear to me why factors of 0.5 and 1.5 have been chosen. If the distribution of zenith optical depth is split into two equal parts by projected area, I expect the denser region to correspond to a core of radius $r/\sqrt{2}$ excised from a sphere of radius r. In this case I think the core will contain about 65% of the volume of the sphere and so the same fraction of the total leaf area. I would therefore expect the proportions to be 0.707 and 1.293, not 0.5 and 1.5.

REPLY 3. We have now reminded the reader that b and c have the same area, and removed the implication that the following argument works only for an LAI of 5. The reviewer is right that the factors have been computed incorrectly (thank you!). The new factors are now used in the paper, which changes the lines of the figures slightly.

COMMENT 4. Figure 6. Previously, results for both the VIS and NIR regions have been shown. Why is the NIR omitted here? Unless the differences are trivial I would suggest showing this region too.

REPLY 4: We have now added the 2-region and 1-region lines to Figs. 2-5 so the reader can see the effect in all cases, including NIR. This means that Fig. 6 is no longer needed.

COMMENT 5. The authors note (page 13, line 12) that there are large uncertainties in the LAI used in weather and climate models. The underlying datasets are derived from remote sensing, so it would be interesting if the authors could comment on the possible application of their model in the retrieval of LAI. The use of a consistent modelling framework in these two areas would be of considerable value.

REPLY 5. This is now discussed in the final section.

# Fast matrix treatment of 3D radiative transfer in vegetation canopies: SPARTACUS-Vegetation 1.1

Robin J. Hogan[1,2], Tristan Quaife[2], and Renato Braghiere[2]

[1]European Centre for Medium-range Weather Forecasts, Reading, UK.
[2]Department of Meteorology, University of Reading, Reading, UK.

*Correspondence to:* Robin J. Hogan (r.j.hogan@ecmwf.int)

**Abstract.** A fast scheme is described to compute the 3D interaction of solar radiation with vegetation canopies. The canopy is split in the horizontal plane into one clear region and one or more vegetated regions, and the two-stream equations are used for each, but with additional terms representing lateral exchange of radiation between regions that are proportional to the area of the interface between them. The resulting coupled set of ordinary differential equations is solved using the matrix-exponential method. The scheme is compared to solar Monte Carlo calculations for idealized scenes from the 'RAMI4PILPS' intercomparison project, for open forest canopies and shrublands both with and without snow on the ground. Agreement is good in both the visible and infrared: for the cases compared, the root-mean-squared difference in reflectance, transmittance and canopy absorptance is 0.020, 0.038 and 0.033, respectively. The technique has potential application to weather and climate modelling.

## 1 Introduction

The treatment of the interaction of vegetation with solar radiation in weather and climate models varies greatly in complexity. The simplest schemes are concerned only with surface albedo and its impact on near-surface temperature forecasts, and indeed Viterbo and Betts (1999) reported a large improvement in forecasts by the ECMWF model when the use of a fixed snow albedo was modified to account for the much lower albedo that occurs when snow falls in forested areas. Much more sophisticated treatments are used in the dynamic vegetation schemes of many climate models, which need to calculate also the fraction of absorbed photosynthetically active radiation (faPAR). But it was reported by Loew et al. (2014) that even state-of-the-art models, when evaluated in benchmarks for which a full physical description of the vegetation was available, had worst-case albedo errors in excess of 0.3. The challenge is to represent the complex 3D structure of vegetation canopies with a radiative transfer algorithm that is nonetheless computationally efficient enough to use in a global model.

Sellers (1985) took the two-stream equations used in atmospheric radiative transfer and applied them to a vegetation canopy. In this approach, the vegetation is treated as a single horizontally homogeneous layer, and a set of three coupled ordinary differential equations are solved for the direct downwelling irradiance and the downwelling and upwelling diffuse irradiances. If the leaves can be assumed randomly oriented then the optical depth of the layer is equal to half the leaf area index (LAI). Meador and Weaver (1980) provided an analytic solution to these equations that is still used in a number of state-of-the-art surface energy exchange schemes (e.g., Best et al., 2011). The first-order error that arises is due to the fact that vegetation canopies are not homogeneous: the heterogeneous distribution of leaves within a tree crown and crowns within a forest stand is such that leaves are more likely to be shadowed by other leaves than if they were homogeneously distributed. Typically this is treated by introducing a 'clumping factor' that scales down the LAI used in the two-stream scheme. A very similar approach has previously been used in atmospheric radiation schemes to treat the clumpiness of clouds (Tiedtke, 1996). The clumping factor for vegetation is typically parameterized as an empirical function of properties of the vegetation and solar zenith angle (e.g., Ni-Meister et al., 2010), but this lacks a physical basis and fails to represent horizontal fluxes into and out of individual tree crowns.

Pinty et al. (2006) described one of the most sophisticated yet affordable schemes to date that attempts to overcome these limitations. Their scheme sums three terms: the reflection from the vegetation assuming a black underlying surface, the reflection from the surface assuming no interaction with the vegetation, and a term representing interactions between the surface and the vegetation. Despite much improved performance compared to the Sellers (1985) scheme, their approach still uses an empirical clumping factor, and is underpinned by the Meador and Weaver (1980) solution that assumes horizontally homogeneous vegetation.

In this paper we exploit recent advances in the atmospheric literature, and adapt the 'SPARTACUS' (SPeedy Algorithm for Radiative Transfer through CloUd Sides) method of Hogan et al. (2016) to the vegetation problem. As described in section 2, this approach employs an explicit description of the horizontal distribution of vegetation for which we can write down a modified version of the two-stream equations that includes terms for lateral radiation exchange between tree crowns and the clear regions between them. The equations are then solved exactly using the matrix-exponential method. This avoids the need for an empirical clumping factor or the Meador and Weaver (1980) solution. In section 3 it is compared to Monte Carlo calculations in idealized forest and shrubland conditions.

## 2 Method

### 2.1 Overview

We use a simple geometrical description of the problem, as shown in Fig. 1. Leafy vegetation is assumed to occupy a single constant-thickness 'canopy layer', with the horizontal domain (corresponding to a weather- or climate-model gridbox) divided into $m$ 'regions'. Within an individual region, the optical properties of the atmosphere and any vegetation are assumed horizontally and vertically homogeneous. Figure 1 considers three regions: one clear (denoted $a$) and two vegetated (denoted $b$ and $c$). The use of two vegetated regions adds the flexibility to represent horizontally heterogeneous tree crowns and trees of differing leaf density, borrowing the idea of Shonk and Hogan (2008) for representing cloud heterogeneity. In section 3 we compare this to a simpler two-region approach with only one vegetated region (denoted $b$). While the tree crowns are depicted in Fig. 1 as cylinders, this is not explicitly assumed; rather, we assume that (1) all azimuthal orientations of the interface between the clear and vegetated regions are equally likely, and (2) the tree crowns are randomly distributed. To represent forests with a significant separation between the ground and the base of the tree crowns, an additional 'sub-canopy layer' may be added, also

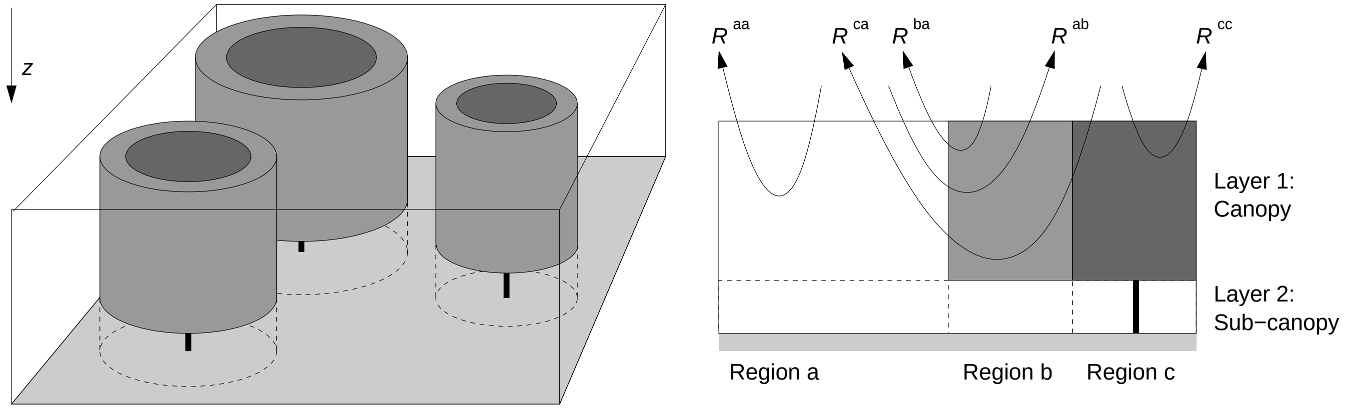


**Figure 1.** Schematic of the idealized vegetation considered in this paper, illustrating the meanings of Layers 1 and 2 and Regions $a$, $b$ and $c$. The diagram on the right also illustrates the interpretation of the elements of the reflectance matrix $\mathbf{R}$ given in (24).

divided into $m$ regions (see Fig. 1). Thus we require as a minimum just four numbers to define the geometry of the problem: the fractional area of the domain covered by vegetation, $c_v$, the vertical depth of the canopy layer, $\Delta z_1$, the vertical depth of the sub-canopy layer, $\Delta z_2$ (which may be zero), and the length of the interface between the clear and vegetated regions per unit area of the domain, $L^{ab}$. Note that although this paper considers only up to two layers and three regions, which is an appropriate level of complexity for a weather or climate model, for other applications additional layers and regions may be added. This would enable the representation of different types of vegetation of different heights, or vegetation in the understory.

In the SPARTACUS method, the two-stream differential equations are used in each region, but with additional terms representing lateral radiation transport between regions. The formulation of these equations is given in section 2.2, with the coefficients to be used in the case of vegetation defined in section 2.3. Section 2.4 then outlines how the $L^{ab}$ term could be parameterized in a model. Section 2.5 describes how the equations are solved for a single layer using matrix exponentials, and section 2.6 describes the use of the adding method to compute the direct and diffuse albedos of the entire scene (vegetation and the surface beneath it). In the context of a weather or climate model, this could be done for the same spectral intervals as the atmospheric radiation scheme, or in the smaller number of broader spectral intervals for which optical properties of the vegetation and surface are defined. These albedos would then be used as boundary conditions for the calculation of the radiative flux profile in the atmosphere above. The downwelling direct and diffuse irradiances output from the atmospheric radiation scheme are then used in section 2.7 to compute the irradiance profile within the vegetation canopy, enabling the absorbed and transmitted radiation to be computed. The appendix describes how the scheme may be made computationally faster by optimizing the treatment of the sub-canopy layer.

### 2.2 Differential two-stream equations in matrix form

This section summarizes the theoretical background to SPARTACUS that was introduced by Hogan et al. (2016). Solar radiation in a particular spectral interval is described by three streams: the diffuse upwelling irradiance ($\mathbf{u}$), the diffuse downwelling irradiance ($\mathbf{v}$) and the direct downwelling irradiance ($\mathbf{s}$), where $\mathbf{u}$ and $\mathbf{v}$ are irradiances into a horizontal plane while $\mathbf{s}$ is into a plane oriented perpendicular to the sun. At any given height, these are column vectors containing the irradiances in $m$ regions; in the equations that follow we use $m = 3$ to match the schematic shown in Fig. 1, but it is straightforward to reduce to two regions. Thus for upwelling irradiance we have $\mathbf{u} = \begin{pmatrix} u^a & u^b & u^c \end{pmatrix}^T$, where each irradiance component is defined as the radiative power divided by the area of the entire gridbox, such that the domain-mean irradiance is obtained by summing the elements of the vector.

The two-stream equations form a set of coupled differential equations that can be written in matrix form as

$$\frac{d}{dz}\begin{pmatrix} \mathbf{u} \\ \mathbf{v} \\ \mathbf{s} \end{pmatrix} = \mathbf{\Gamma}\begin{pmatrix} \mathbf{u} \\ \mathbf{v} \\ \mathbf{s} \end{pmatrix}, \tag{1}$$

where $z$ is height measured *downward* from the top of the layer, and $\mathbf{\Gamma}$ is a matrix describing the interactions between irradiance components and between different regions. It is convenient to partition it into a set of $m \times m$ component matrices as follows:

$$\mathbf{\Gamma} = \begin{pmatrix} -\mathbf{\Gamma}_1 & -\mathbf{\Gamma}_2 & -\mathbf{\Gamma}_3 \\ \mathbf{\Gamma}_2 & \mathbf{\Gamma}_1 & \mathbf{\Gamma}_4 \\ & & \mathbf{\Gamma}_0 \end{pmatrix}, \tag{2}$$

where

$$\mathbf{\Gamma}_0 = \begin{pmatrix} -\sigma_0^a/\mu_0 & & \\ & -\sigma_0^b/\mu_0 & \\ & & -\sigma_0^c/\mu_0 \end{pmatrix} + \begin{pmatrix} -f_{\mathrm{dir}}^{ab} & +f_{\mathrm{dir}}^{ba} & \\ +f_{\mathrm{dir}}^{ab} & -f_{\mathrm{dir}}^{ba} - f_{\mathrm{dir}}^{bc} & +f_{\mathrm{dir}}^{cb} \\ & +f_{\mathrm{dir}}^{bc} & -f_{\mathrm{dir}}^{cb} \end{pmatrix}; \tag{3}$$

$$\mathbf{\Gamma}_1 = \begin{pmatrix} -\sigma^a\gamma_1^a & & \\ & -\sigma^b\gamma_1^b & \\ & & -\sigma^c\gamma_1^c \end{pmatrix} + \begin{pmatrix} -f_{\mathrm{diff}}^{ab} & +f_{\mathrm{diff}}^{ba} & \\ +f_{\mathrm{diff}}^{ab} & -f_{\mathrm{diff}}^{ba} - f_{\mathrm{diff}}^{bc} & +f_{\mathrm{diff}}^{cb} \\ & +f_{\mathrm{diff}}^{bc} & -f_{\mathrm{diff}}^{cb} \end{pmatrix}; \tag{4}$$

$$\mathbf{\Gamma}_2 = \begin{pmatrix} \sigma^a\gamma_2^a & & \\ & \sigma^b\gamma_2^b & \\ & & \sigma^c\gamma_2^c \end{pmatrix}; \tag{5}$$

$$\mathbf{\Gamma}_3 = \begin{pmatrix} \sigma^a\omega^a\gamma_3^a & & \\ & \sigma^b\omega^b\gamma_3^b & \\ & & \sigma^c\omega^c\gamma_3^c \end{pmatrix}, \tag{6}$$

and $\mathbf{\Gamma}_4$ is the same as $\mathbf{\Gamma}_3$ but using the quantity $\gamma_4$ in place of $\gamma_3$. Missing entries in all these matrices are taken to be zero. The $\mathbf{\Gamma}_0$ and $\mathbf{\Gamma}_1$ matrices describe the rate at which the direct and diffuse downwelling irradiances, respectively, change along their path. They are expressed in (3) and (4) as the sum of two matrices: the first matrix in each case represents losses due to scattering and absorption, while the second represents exchange of radiation between regions. The $\mathbf{\Gamma}_2$ matrix describes the rate of scattering of diffuse radiation from one direction to the other, while the $\mathbf{\Gamma}_3$ and $\mathbf{\Gamma}_4$ matrices describe the rate at which the direct solar beam is scattered into the upwelling and downwelling diffuse streams. The minus signs in front of the matrices on the top row of (2) are due to this line corresponding to upwelling radiation, but the vertical coordinate increasing downward.

The symbols in (3) to (6) have the following meanings. The extinction coefficient to diffuse radiation of region $j$ is denoted $\sigma^j$, and $\sigma_0^j$ is the same but for direct radiation. The distinction between the two permits the flexibility to represent leaves with a preferred orientation. The cosine of the solar zenith angle is denoted $\mu_0$ while the single-scattering albedo is $\omega$. The coefficients $\gamma_1$–$\gamma_4$ govern the exchange of radiation between the three streams. Finally, the coefficients $f_{\mathrm{dir}}^{jk}$ and $f_{\mathrm{diff}}^{jk}$ represent the rate at which direct and diffuse radiation, respectively, is transferred from region $j$ to region $k$. All these symbols are defined in terms of physical properties of the scene in the next section.

### 2.3 Coefficients in the two-stream equations

The matrix form of the two-stream equations in section 2.2 introduced several coefficients that are themselves functions of more fundamental optical or geometric properties. The $\gamma_1$–$\gamma_4$ coefficients may be written as (Meador and Weaver, 1980):

$$\gamma_1 = [1 - \omega(1-\beta)]/\mu_1; \tag{7}$$

$$\gamma_2 = \omega\beta/\mu_1; \tag{8}$$

$$\gamma_3 = \beta_0; \tag{9}$$

$$\gamma_4 = 1 - \beta_0, \tag{10}$$

where $\beta$ and $\beta_0$ are the ‘upscatter’ fractions, the fractions of downwelling radiation (in the diffuse and direct streams respectively) that are scattered upward, and $\mu_1$ is the cosine of the effective zenith angle of diffuse radiation. For the remainder of this paper we assume the diffuse radiation to be hemispherically isotropic, so $\mu_1 = 1/2$.

In the simplest case where leaves are assumed to be randomly oriented, the optical depth of a region is equal to half its LAI, and therefore for a layer of thickness $\Delta z$, the extinction coefficients to direct and diffuse radiation are the same and are given by

$$\sigma = \sigma_0 = \mathrm{LAI}/(2\Delta z). \tag{11}$$

Assuming the leaves to be bi-Lambertian scatterers with reflectance $r$ and transmittance $t$, the single scattering albedo is given by

$$\omega = r + t, \tag{12}$$

and the upscatter fractions by

$$\beta = 1/2 + \mu_1(r - t)/(3\omega); \tag{13}$$

$$\beta_0 = 1/2 + \mu_0(r - t)/(3\omega). \tag{14}$$

These last two formulas may be derived by equating (8) and (9) with the definitions given in the lowest row of Table 4 of Pinty et al. (2006). Pinty et al. (2006) also provided more general expressions for leaves with a preferential alignment.

The rates of lateral exchange of radiation between regions that appear in (3) and (4) may be derived from geometrical arguments (Hogan and Shonk, 2013; Schäfer et al., 2016) as

$$f^{ij}_{\mathrm{diff}} = L^{ij}/(2c^i); \tag{15}$$

$$f^{ij}_{\mathrm{dir}} = L^{ij}\tan(\theta_0)/(\pi c^i), \tag{16}$$

where $\theta_0$ is the solar zenith angle, $L^{ij}$ is the length of the interface between regions $i$ and $j$ per unit area of the horizontal domain, and $c^i$ is the fractional area of the domain covered by region $i$. In the $m = 3$ case we have two regions to represent horizontal heterogeneity of zenith optical depth, and following the findings of Shonk and Hogan (2008) we assume them to be of equal area, i.e. $c^b = c^c = c_v/2$ and $c^a = 1 - c_v$ (where $c_v$ is the fractional coverage of vegetation). This leads to $f^{bc}_{\mathrm{dir}} = f^{cb}_{\mathrm{dir}}$ and $f^{bc}_{\mathrm{diff}} = f^{cb}_{\mathrm{diff}}$.

Lastly in this section, we consider how to represent the effect of vertical tree trunks in region $c$ of the sub-canopy layer (as illustrated in Fig. 1). If the trunks are of a size and number such that a horizontal slice through the sub-canopy layer intercepts a normalized total trunk perimeter (per unit area of region $c$) of $L_t$, then by analogy with (15) and (16), the diffuse and direct extinction coefficients are given by

$$\sigma = L_t/(2c^c); \tag{17}$$

$$\sigma_0 = L_t\tan(\theta_0)/(\pi c^c). \tag{18}$$

For simplicity we assume the trunks to be Lambertian reflectors, in which case $\omega$ is simply the trunk albedo, and with no preference for upward or downward scattering we have $\beta = \beta_0 = 1/2$.

Now that the problem has been formulated mathematically, we can explain how the assumption that the tree crowns are randomly distributed is implicitly encoded in the equations. At any given height in the canopy layer, the probability of direct radiation in the clear region intercepting a tree crown, per unit distance travelled vertically, is $f^{ab}_{\mathrm{dir}}$. This factor is constant in the canopy layer. Therefore, for direct radiation emerging unscattered from the edge of a tree crown into the clear region, the fraction of that light remaining in the clear region rather than having encountered another tree varies in proportion to $\exp(-f^{ab}_{\mathrm{dir}}z)$, where $z$ is the vertical distance travelled in the clear region (assuming no absorption or scattering, and that the light remains within the canopy layer). To express this in terms of horizontal distance $x$, we use (16) and recognize that $\tan(\theta_0) = x/z$ to obtain $\exp[-xL^{ab}/(\pi c^a)]$. This implies that the chord lengths between the edges of tree crowns in all possible horizontal directions also follow the same exponential distribution, which in turn defines the spatial distribution of trees as random.

### 2.4 Parameterizing the vegetation perimeter length

The length of the vegetation–clear boundary, $L^{ab}$, is the fundamental property used by SPARTACUS to characterize the importance of lateral radiative exchange between clear and vegetated regions. It is therefore the quantity that would ideally be measured in field experiments. However, in the context of weather and climate modelling, the physiographic variable available would most likely be vegetation cover $c_v$ (e.g. from the measurements of Hansen et al., 2003), and $L^{ab}$ would need to be parameterized as a function of $c_v$. This can be done by introducing an extra parameter representing the characteristic size of a tree crown that is independent of $c_v$. We now present two possible characteristic sizes that could be used.

In the first case, we define the *effective tree diameter*, $D$, to be the diameter of identical, cylindrical and *physically separated* tree crowns in an idealized forest with the same $L^{ab}$ and $c_v$ as the real forest. The assumption that tree crowns do not touch was used by Widlowski et al (2011) in generating the idealized scenes that we use in section 3 to evaluate SPARTACUS. The phenomenon of the crowns of some tree species remaining separate even for large tree cover is known as *crown shyness* (e.g. Putz et al., 1984). In analogy to the concept of an effective cloud diameter by Jensen et al. (2008), this leads to the definition

$$L^{ab} = 4c_v/D. \tag{19}$$

If region $c$ represents the central core of the tree crowns, as depicted in Fig. 1, then this implies $L^{bc} = L^{ab}/\sqrt{2}$.

In the second case we assume that tree crowns can touch each other, and will do so increasingly in dense forests. This behaviour is represented by defining an *effective tree scale*, $S$, such that

$$L^{ab} = 4c_v(1 - c_v)/S. \tag{20}$$

This form is inspired by the idealized geometrical analysis of Morcrette (2012): if we place idealized trees with a square footprint measuring $S \times S$ randomly on a grid, then on average the normalized perimeter length $L^{ab}$ will follow (20). It leads to the behaviour that $L^{ab}$ increases with $c_v$ up to $c_v = 1/2$, but for further increases in $c_v$, crown touching dominates which causes $L^{ab}$ to reduce again.

In the field we would envisage measuring $L^{ab}$ and $c_v$ and then using (19) and (20) to infer $D$ and $S$. The characteristic size that varies least with $c_v$ would then be the one best suited for use in a weather or climate model, and potentially a constant characteristic size could be used to characterize an entire forest on a regional scale. Within individual gridboxes of the model, it would be used to compute $L^{ab}$ from $c_v$ using either (19) or (20).

### 2.5 Solution to equations within one layer

We may write the solution to (1) in terms of a matrix exponential (Waterman, 1981; Hogan et al., 2016): the irradiances at the base of a layer of thickness $\Delta z$ are related to the irradiances at the top of the layer via

$$\begin{pmatrix} \mathbf{u} \\ \mathbf{v} \\ \mathbf{s} \end{pmatrix}_{z=z+\Delta z} = \exp(\mathbf{\Gamma}\Delta z) \begin{pmatrix} \mathbf{u} \\ \mathbf{v} \\ \mathbf{s} \end{pmatrix}_{z=z}, \tag{21}$$

where the matrix exponential may be computed numerically using the scaling and squaring method (e.g. Higham, 2005). If 3D radiative transfer is neglected then $f_{\mathrm{diff}} = f_{\mathrm{dir}} = 0$, which decouples the equations to the extent that a computationally cheaper analytical solution is possible (Meador and Weaver, 1980). Conversely, if scattering and absorption are ignored but 3D radiative transfer is retained, a reasonable assumption in the sub-canopy layer, then $\sigma = \sigma_0 = 0$, which also decouples the equations and leads to the computationally cheaper solution given in the appendix.

In order to compute the irradiance profile, we wish to work with expressions of the following form:

$$\mathbf{u}(z) = \mathbf{T}\mathbf{u}(z+\Delta z) + \mathbf{R}\mathbf{v}(z) + \mathbf{S}^{+}\mathbf{s}(z); \tag{22}$$

$$\mathbf{v}(z+\Delta z) = \mathbf{T}\mathbf{v}(z) + \mathbf{R}\mathbf{u}(z+\Delta z) + \mathbf{S}^{-}\mathbf{s}(z), \tag{23}$$

where (22) states that the upwelling irradiance exiting the top of the layer is equal to transmission of the upwelling irradiance entering the base of the layer, plus reflection of the downwelling irradiance entering the top of the layer, plus scattering of the direct solar irradiance entering the top of the layer; and similarly for (23). Figure 1 illustrates the meaning of the elements of the diffuse reflectance matrix $\mathbf{R}$ for the canopy layer:

$$\mathbf{R} = \begin{pmatrix} R^{aa} & R^{ba} & R^{ca} \\ R^{ab} & R^{bb} & R^{cb} \\ R^{ac} & R^{bc} & R^{cc} \end{pmatrix}, \tag{24}$$

where $R^{ij}$ is the fraction of diffuse downwelling radiation entering the top of region $i$ that is scattered out of the top of region $j$ without exiting the base of the layer. The other matrices have analogous definitions: $\mathbf{T}$ represents the transmission of diffuse radiation across the layer, and $\mathbf{S}^{+}$ and $\mathbf{S}^{-}$ represent the scattering of radiation from the direct downwelling stream at the top of the layer to the diffuse upwelling stream at the top of the layer and the diffuse downwelling stream at the base of the layer, respectively.

These matrices may be derived from the matrix exponential, which we decompose into seven $m \times m$ matrices:

$$\exp(\mathbf{\Gamma}\Delta z) = \begin{pmatrix} \mathbf{E}_{uu} & \mathbf{E}_{uv} & \mathbf{E}_{us} \\ \mathbf{E}_{vu} & \mathbf{E}_{vv} & \mathbf{E}_{vs} \\ & & \mathbf{E}_{0} \end{pmatrix}. \tag{25}$$

It was shown by Hogan et al. (2016) that

$$\mathbf{R} = -\mathbf{E}_{uu}^{-1}\mathbf{E}_{uv}; \tag{26}$$

$$\mathbf{T} = \mathbf{E}_{vu}\mathbf{R} + \mathbf{E}_{vv}; \tag{27}$$

$$\mathbf{S}^{+} = -\mathbf{E}_{uu}^{-1}\mathbf{E}_{us}; \tag{28}$$

$$\mathbf{S}^{-} = \mathbf{E}_{vu}\mathbf{S}^{+} + \mathbf{E}_{vs}. \tag{29}$$

Moreover, the direct irradiance exiting the base of a layer is computed from the direct irradiance entering the top of a layer via $\mathbf{s}(z+\Delta z) = \mathbf{E}_0\mathbf{s}(z)$.

### 2.6 Extension to multiple layers

To compute the irradiance profile we use the adding method (Lacis and Hansen, 1974) but in a somewhat different form to Hogan et al. (2016), in order to facilitate integration within a full atmospheric radiation scheme. This section considers the first part: stepping up through the vegetation layers computing the albedo of the scene below each layer interface. We define the matrix $\mathbf{A}_{i+1/2}$ as the albedo to diffuse downwelling radiation of the scene below interface $i+1/2$ (including the surface contribution), and the matrix $\mathbf{D}_{i+1/2}$ as the albedo to direct radiation. The off-diagonal terms of these matrices represent the fraction of radiation downwelling in one region that is reflected back into the other. At the surface (interface $n+1/2$ for an $n$-layer description of the canopy), these matrices are diagonal:

$$\mathbf{A}_{n+1/2} = \begin{pmatrix} \alpha_{\mathrm{diff}}^{a} & & \\ & \alpha_{\mathrm{diff}}^{b} & \\ & & \alpha_{\mathrm{diff}}^{c} \end{pmatrix}; \tag{30}$$

$$\mathbf{D}_{n+1/2} = \mu_0 \begin{pmatrix} \alpha_{\mathrm{dir}}^{a} & & \\ & \alpha_{\mathrm{dir}}^{b} & \\ & & \alpha_{\mathrm{dir}}^{c} \end{pmatrix}, \tag{31}$$

where for maximum flexibility we allow for separate direct and diffuse surface albedos, and separate albedos below each region to represent lower snow cover beneath trees.

We then use the adding method to compute $\mathbf{A}$ and $\mathbf{D}$ just below the interface above, accounting for the possibility of multiple scattering. In the case of the diffuse albedo matrix we have

$$\begin{aligned}\mathbf{A}_{i-1/2} = \mathbf{R}_i + \mathbf{T}_i &\left[\mathbf{I} + \mathbf{A}_{i+1/2}\mathbf{R}_i + (\mathbf{A}_{i+1/2}\mathbf{R}_i)^2 + \cdots\right] \\ &\times \mathbf{A}_{i+1/2}\mathbf{T}_i,\end{aligned} \tag{32}$$

where $\mathbf{I}$ is the $m \times m$ identity matrix. This equation states that the albedo at interface $i-1/2$ is equal to the reflection of layer $i$, plus the albedo at interface $i+1/2$ accounting for the two-way transmission through the intervening layer. The term in square brackets accounts for multiple scattering between interface $i+1/2$ and layer $i$, and since it is a geometric series of matrices, the equation reduces to

$$\mathbf{A}_{i-1/2} = \mathbf{R}_i + \mathbf{T}_i \left(\mathbf{I} - \mathbf{A}_{i+1/2}\mathbf{R}_i\right)^{-1} \mathbf{A}_{i+1/2}\mathbf{T}_i. \tag{33}$$

Similarly, the direct albedo matrix at the interface above is given by

$$\mathbf{D}_{i-1/2} = \mathbf{S}_i^+ + \mathbf{T}_i \left(\mathbf{I} - \mathbf{A}_{i+1/2}\mathbf{R}_i\right)^{-1} \times \left(\mathbf{D}_{i+1/2}\mathbf{E}_{0i} + \mathbf{A}_{i+1/2}\mathbf{S}_i^-\right), \tag{34}$$

where $\mathbf{D}_{i+1/2}\mathbf{E}_{0i}$ represents the direct radiation that passes down through layer $i$ without being scattered and is then reflected up from interface $i+1/2$, while $\mathbf{A}_{i+1/2}\mathbf{S}_i^-$ represents direct radiation that is scattered into the downward diffuse stream in layer $i$ and then reflected up from interface $i+1/2$. For the two-layer description of the vegetation shown in Fig. 1, (33) and (34) are applied first at interface 1.5 (between the canopy and the sub-canopy layers) and then at interface 0.5 (the top of the canopy). It is straightforward to add additional layers.

At this point we are able to compute the scalar 'scene albedos' of the surface and the vegetation. Denoting $\mathbf{c} = \begin{pmatrix} c^a & c^b & c^c \end{pmatrix}^T$ as a column vector containing the area fractions of each region, the scene albedos to diffuse and direct radiation are

$$\alpha_{\mathrm{diff,scene}} = \mathbf{c}^T\mathbf{A}_{1/2}\mathbf{c}; \tag{35}$$

$$\alpha_{\mathrm{dir,scene}} = \mathbf{c}^T\mathbf{D}_{1/2}\mathbf{c}. \tag{36}$$

When implementing the scheme described in this paper in the radiation scheme of a weather or climate model, these albedos would be used as the boundary conditions for the computation of the irradiance profile through the atmosphere.

### 2.7 Computing irradiances within the canopy

After running the atmospheric part of the radiation scheme, we proceed down through the vegetation to compute the direct and diffuse irradiances at each interface, ending up at the surface. The output from the atmospheric radiation calculation includes the downwelling direct and diffuse irradiances at the top of the canopy, $s_{1/2}$ and $v_{1/2}$. These are partitioned into component irradiances at the top of each region according to the area fraction of each region:

$$\mathbf{s}_{1/2} = s_{1/2}\mathbf{c}; \tag{37}$$

$$\mathbf{v}_{1/2} = v_{1/2}\mathbf{c}. \tag{38}$$

The direct irradiance is propagated down through the vegetation simply with

$$\mathbf{s}_{i+1/2} = \mathbf{E}_{0i}\mathbf{s}_{i-1/2}. \tag{39}$$

The diffuse irradiances at the interface beneath satisfy

$$\mathbf{u}_{i+1/2} = \mathbf{A}_{i+1/2}\mathbf{v}_{i+1/2} + \mathbf{D}_{i+1/2}\mathbf{s}_{i+1/2}; \tag{40}$$

$$\mathbf{v}_{i+1/2} = \mathbf{T}_i\mathbf{v}_{i-1/2} + \mathbf{R}_i\mathbf{u}_{i+1/2} + \mathbf{S}_i^-\mathbf{s}_{i-1/2}. \tag{41}$$

**Table 1.** Variables describing the geometry of 'Open forest' and 'Shrubland' RAMI4PILPS scenarios simulated in this paper (see Widlowski et al, 2011). The Leaf Area Index of a vegetated region is defined as the total leaf surface area divided by the downward projected area of the region.

| Variable | Symbol | Open forest | Shrubland |
|---|---|---|---|
| Leaf Area Index of vegetated region | LAI | 5 | 2.5 |
| Area fraction of vegetated region | $c_v$ | 0.1, 0.3, 0.5 | 0.1, 0.2, 0.4 |
| Effective tree diameter | $D$ | 10 m | 1 m |
| Canopy layer depth | $\Delta z_1$ | 10 m | 1 m |
| Sub-canopy layer depth | $\Delta z_2$ | 4 m | 0.01 m |

Eliminating $\mathbf{u}_{i+1/2}$ yields

$$\mathbf{v}_{i+1/2} = \left(\mathbf{I} - \mathbf{R}_i \mathbf{A}_{i+1/2}\right)^{-1} \times \left(\mathbf{T}_i \mathbf{v}_{i-1/2} + \mathbf{R}_i \mathbf{D}_{i+1/2} \mathbf{s}_{i+1/2} + \mathbf{S}_i^- \mathbf{s}_{i-1/2}\right). \quad (42)$$

Thus, application of (42) followed by (40) provides the irradiances at the interface below.

The horizontally averaged upwelling diffuse, downwelling diffuse and downwelling direct irradiances at interface $i+1/2$, denoted $u_{i+1/2}$, $v_{i+1/2}$ and $s_{i+1/2}$, respectively, are found by simply summing the elements of $\mathbf{u}_{i+1/2}$, $\mathbf{v}_{i+1/2}$ and $\mathbf{s}_{i+1/2}$. The total downwelling irradiance is then the sum of the direct and diffuse components: $d_{i+1/2} = \mu_0 s_{i+1/2} + v_{i+1/2}$. The solar absorption by each layer is the difference in net irradiance between the interface above and below it. These definitions are used to compute normalized quantities that will be used to evaluate SPARTACUS in section 3.

## 3 Results

To test the application of the SPARTACUS methodology to the vegetation problem, we use two 3D scenarios from the RAMI4PILPS[1] intercomparison exercise (Widlowski et al, 2011). The first scenario is an idealized representation of an open forest canopy, and consists of spheres of leafy vegetation of diameter 10 m, while the second represents shrubland and consists of spheres of diameter 1 m. Details are provided in Table 1, including the three different area coverages of vegetation that are used. Two spectral intervals are simulated, representing the photosynthetically-active visible region and the near-infrared, and both snow-free and snow-covered surfaces are considered. Table 2 lists the optical properties of the leaves and the surfaces in the two spectral intervals.

All combinations have been simulated using the three-region ($m = 3$) version of SPARTACUS. The two vegetated regions ($b$ and $c$) are of equal projected area and are configured to approximate the distribution of zenith optical depth of spheres. So for a sphere of radius $r$, region $c$ represents the upper half of the optical depth distribution corresponding to a core of radius

[1] RAMI is the Radiation Transfer Model Intercomparison, and PILPS is the Project for Intercomparison of Land surface Parameterization Schemes.

**Table 2.** Variables describing the optical properties of the leaves and the surface in the visible and near-infrared in the RAMI4PILPS cases (see Widlowski et al, 2011).

| Variable | Symbol | Visible | Near-infrared |
|---|---|---|---|
| Leaf reflectance | $r$ | 0.0735 | 0.3912 |
| Leaf transmittance | $t$ | 0.0566 | 0.4146 |
| Snow-free surface albedo | $\alpha_{\mathrm{med}}$ | 0.1217 | 0.2142 |
| Snow albedo | $\alpha_{\mathrm{snow}}$ | 0.9640 | 0.5568 |

$r/\sqrt{2}$ projected down through the sphere, which contains $1-2^{-3/2}$, or 65%, of its volume. Likewise, region $b$ represents the lower half of the distribution corresponding to the remaining shell, and this contains $2^{-3/2}$, or 35%, of the volume of the sphere. Therefore, if the mean optical depth of the sphere is $\delta$, the mean optical depths of regions $b$ and $c$ are $0.7\delta$ and $1.3\delta$, respectively.

Figure 2 shows the results for the open forest canopy in the visible part of the spectrum while Fig. 3 shows the same but for the near-infrared. The corresponding results for the shrubland scenario are shown Figs. 4 and 5. Using the domain-mean irradiances defined in section 2.7, the quantities shown are reflectance $R$, transmittance $T$ and absorptance $A$:

$$R = u_{1/2}/d_{1/2}; \tag{43}$$

$$T = d_{n+1/2}/d_{1/2}; \tag{44}$$

$$A = \left(d_{1/2} - u_{1/2} - d_{n+1/2} + u_{n+1/2}\right)/d_{1/2}. \tag{45}$$

It can be seen that the 3-region version of SPARTACUS compares well to Monte Carlo, including all four combinations of high- and low-reflectance leaves over a high- or low-reflectance surface. In total we have 72 points of comparison with Monte Carlo calculations: two scenarios, two spectral intervals, two surface types, three vegetation covers and three solar zenith angles. Treating the Monte Carlo as 'truth', we compute that the root-mean-squared error in $R$, $T$ and $A$ is 0.020, 0.038 and 0.033, respectively. Probably the worse performance occurs for low solar zenith angle in Fig. 2f (corresponding to visible radiation illuminating a scene with a tree cover of 0.5 over snow): $A$ is overestimated by around 0.05 suggesting that a little too much reflected sunlight from the snow enters the tree crowns and is absorbed.

We next investigate how the results are degraded when using a more approximate description of the scene. Each panel of Figs. 2–5 includes two further lines. The 'homogeneous' calculation uses the same SPARTACUS code but with only one region, treating the canopy as a single horizontally homogeneous layer with the same leaf area index. This is essentially the same as the Sellers (1985) assumption and indeed with a single region the matrix-exponential method yields the same result as the Meador and Weaver (1980) solution. We see immediately that when the leaves are not clumped into trees but rather distributed uniformly, their exposure to incoming radiation is maximized and their absorptance is overestimated by up to 0.3. Conversely,

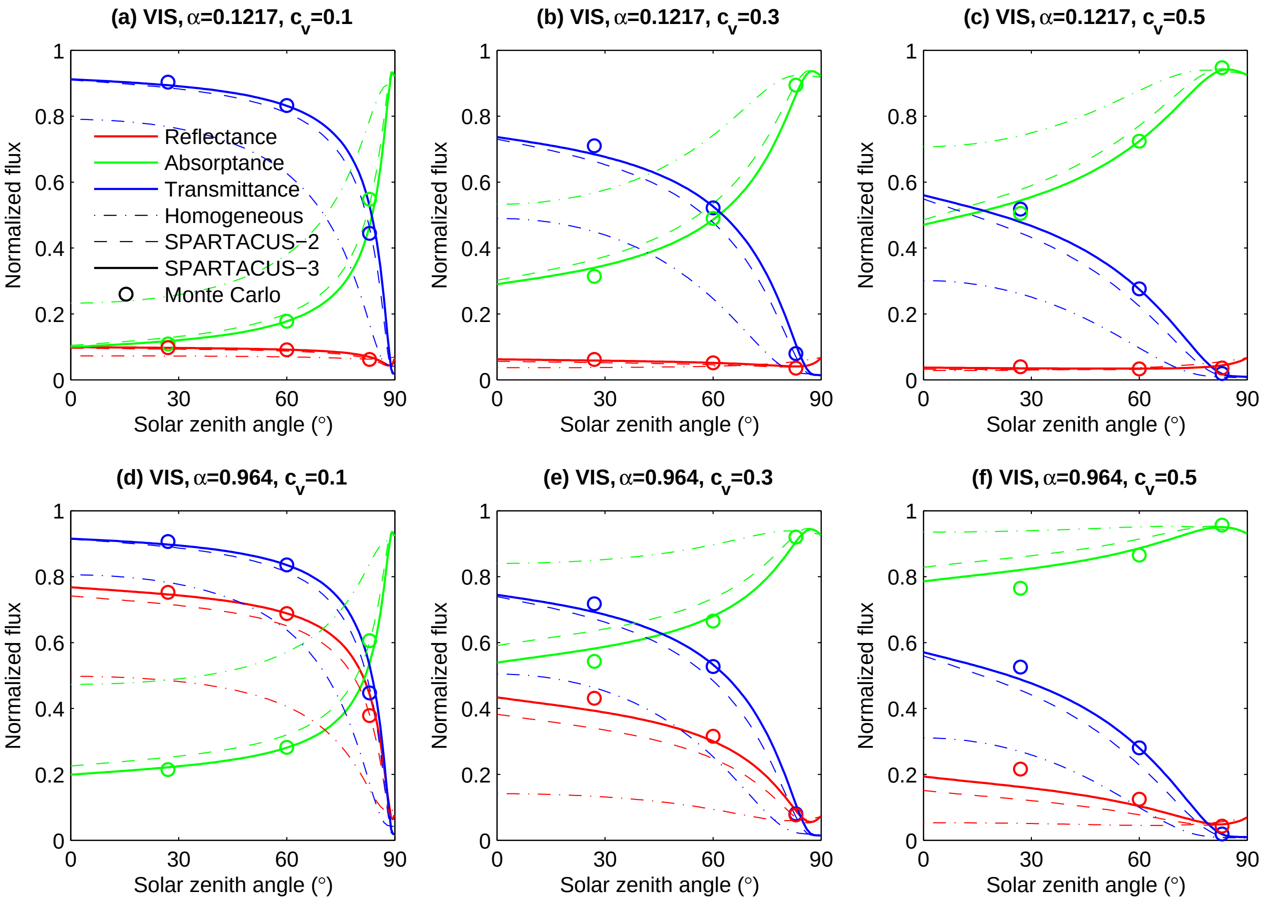


**Figure 2.** Comparison of normalized irradiances versus solar zenith angle for the RAMI4PILPS 'Open forest canopy' scenario with optical properties appropriate for visible radiation. The two rows of panels show results for different surface albedos ($\alpha$) with the top row using values appropriate for a snow-free surface and the bottom row using values for a snow-covered surface. The columns represent different areal tree fractions ($c_v$). The three solid lines depict the reflectance, transmittance and absorptance defined in (43), (44) and (45), computed using the 3-region version of SPARTACUS. The dashed and dot-dashed lines depict the 2-region and 1-region SPARTACUS calculations, respectively, where the latter involves complete horizontal homogenization of the vegetation properties through the domain. Also shown are the corresponding Monte Carlo calculations of Widlowski et al (2011) at solar zenith angles of 27°, 60° and 83°.

both the reflectance and transmittance of the scene are underestimated, with the largest error in reflectance for overhead sun and a snow-covered surface (Fig. 2e).

The 2-region SPARTACUS calculation shown in Figs. 2–5 treats individual trees as horizontally homogeneous cylinders, thereby neglecting the variation in zenith optical depth of the spherical trees simulated by the Monte Carlo calculations. The results are much better than those with just a single region, and virtually the same as the 3-region calculation in the near infrared, but absorption still tends to be overestimated in the visible. An analogous bias occurs in cloudy radiative transfer

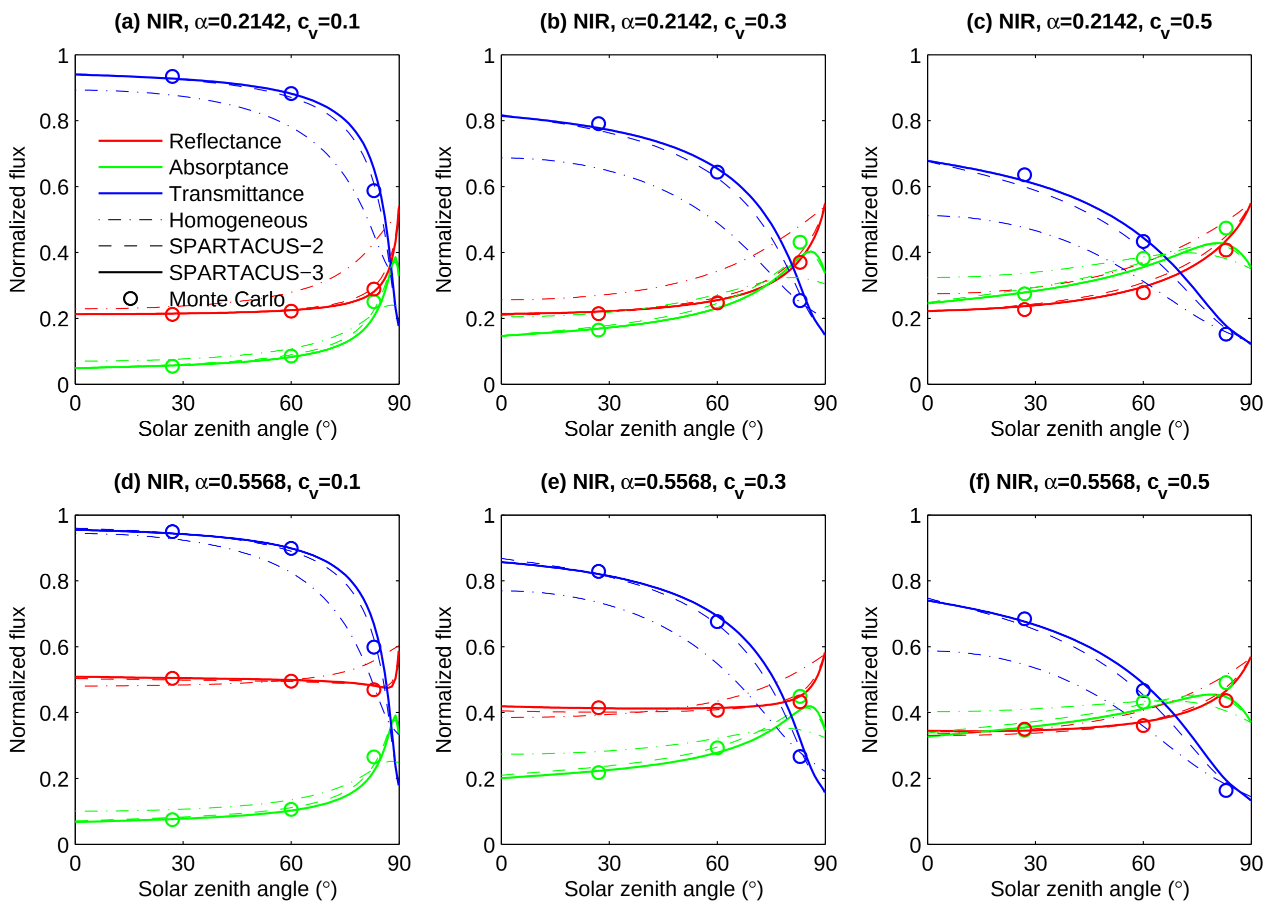


**Figure 3.** As Fig. 2 but with optical properties appropriate for near-infrared radiation.

calculations in which the internal variability of clouds is neglected, which led to the proposal of Shonk and Hogan (2008) to use three regions to represent a partially cloudy scene. The success of the 3-region approach suggests that it is also useful for vegetation. Having said this, the uncertainty in computing radiative transfer the vegetation canopies of weather and climate models is typically dominated by uncertainties in leaf area index. Therefore, for many applications the 2-region calculation would be adequate. Since the computational cost of SPARTACUS is dominated by the matrix exponential calculation, whose cost is approximately proportional to $m^3$, we would expect a 2-region SPARTACUS calculation to be at least 3 times faster than a 3-region calculation.

## 4 Discussion and conclusions

This paper has demonstrated the potential for the interaction of solar radiation and complex vegetation canopies to be represented via an explicit description of the geometry, building on the SPARTACUS algorithm for representing the 3D radiative

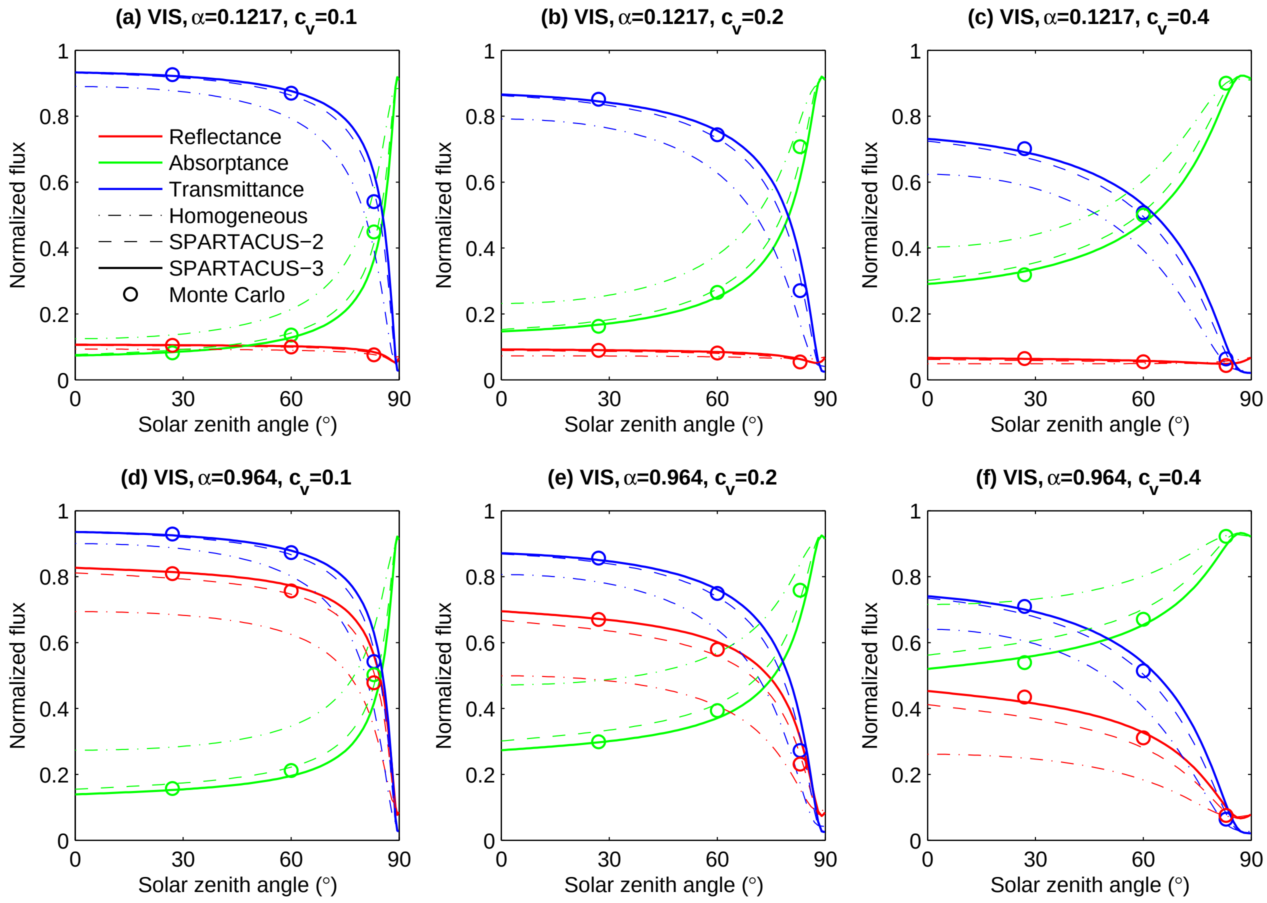


**Figure 4.** As Fig. 2 but for the RAMI4PILPS ‘Shrubland’ scenario.

effects of clouds (Hogan et al., 2016). The two-stream equations are written down for the tree crown and the gaps between them, but with additional terms for the horizontal exchange of radiation between regions. The equations are solved exactly using the matrix exponential method. Multiple layers are possible, although we have simplified the original SPARTACUS algorithm by assuming maximum overlap between the regions in each layer, rather than the arbitrary overlap considered by Hogan et al. (2016). Comparison against Monte Carlo calculations from the RAMI4PILPS intercomparison exercise indicates that canopy reflectance, transmittance and absorptance are computed significantly more accurately than a number of state-of-the-art models assessed by Loew et al. (2014).

An advantage of the SPARTACUS approach is that in addition to LAI, only a handful of physiographic variables are required to describe the geometry of the vegetation, such as the vegetation height, coverage, and the diameter of typical tree crowns. Global estimates of the first two are now available from satellites (e.g., Simard et al., 2011; Hansen et al., 2003).

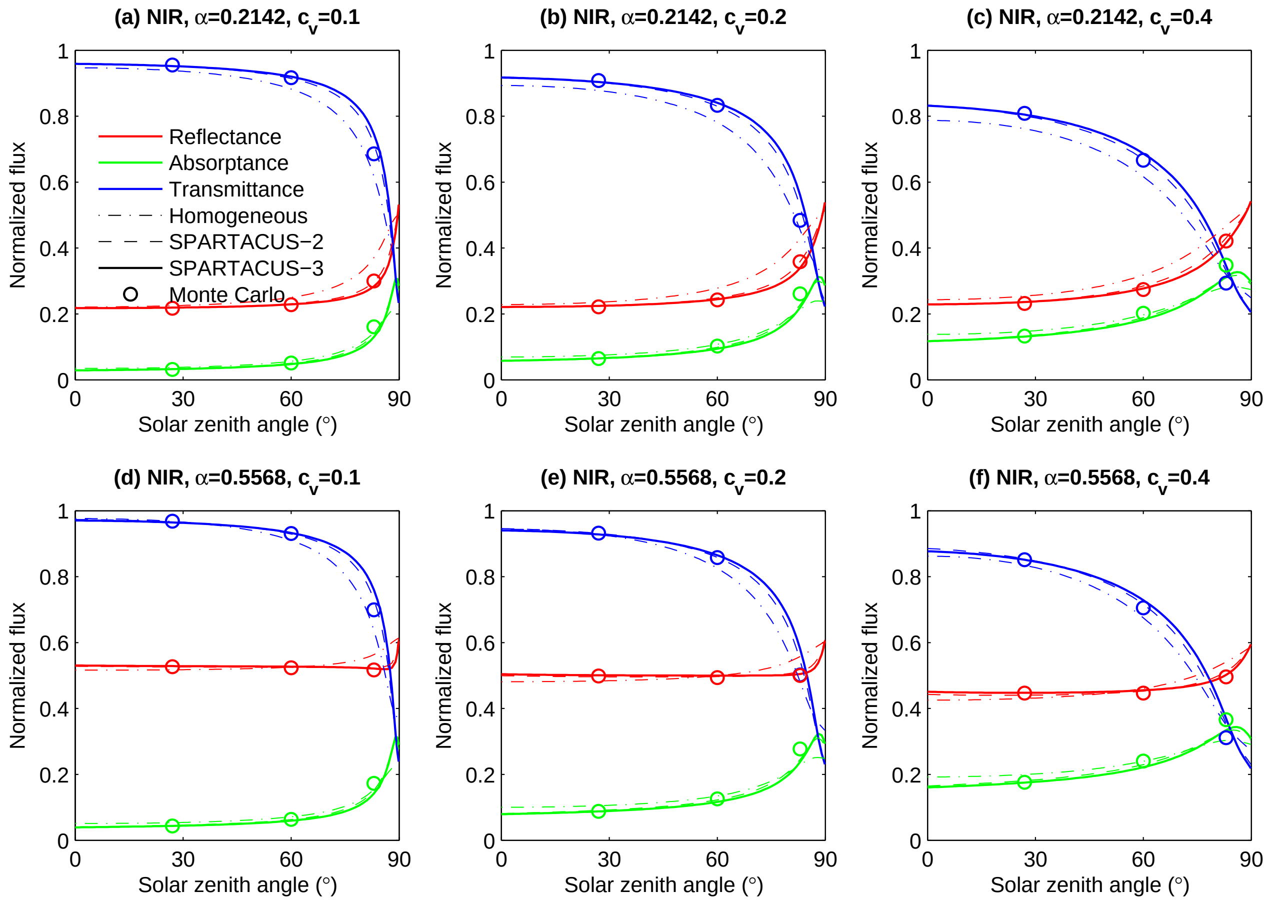


**Figure 5.** As Fig. 4 but with optical properties appropriate for near-infrared radiation.

Although the testing scenarios used in this papers were simple homogeneous spheres with no woody material, the method described has the capability to represent more complex geometries. Horizontal variations in leaf density or tree crowns with different properties may be represented via two or more vegetated regions with distinct optical properties. This paper considered a two-layer description of the vegetation, with a single canopy layer overlying a sub-canopy layer, but the equations can easily be applied to a multi-layer description of the canopy, for example to compute the vertical profile of absorbed photosynthetically active radiation. The optical effects of tree trunks may also be incorporated. Moreover, the good performance with solar radiation suggests that the thermal-infrared version of SPARTACUS (Schäfer et al., 2016) could also be adapted to the vegetation problem.

A further possible extension to SPARTACUS would be to use it for remote sensing; in addition to the possibility of more accurate LAI retrievals via explicit treatment of 3D radiative effects, this would provide a consistent framework for both remote sensing and weather/climate modelling. The challenge would be to adapt SPARTACUS to compute solar radiances rather than irradiances, which adds an extra degree of geometrical complexity. For example, trees cast shadows on the ground, but the extent to which shadows are visible to a satellite depends on the sensor zenith angle and the azimuthal separation of the sensor and the sun.

## Code availability

A Matlab implementation of the algorithm is freely available from http://www.met.reading.ac.uk/clouds/spartacus, and was used to produce Figs. 2–5. Work is in progress to implement the algorithm in the 'ecRad' atmospheric radiation scheme (Hogan and Bozzo, 2016).

## Appendix A: Faster treatment of clear layers

The main role of the sub-canopy layer is to represent how much of the sunlight passing down between the trees is reflected back up into the base of a tree crown, i.e. the off-diagonal elements of $\mathbf{A}_{n-1/2}$ and $\mathbf{D}_{n-1/2}$. Since the matrix exponential accounts for most of the cost of the scheme, if we can accelerate or approximate the treatment of the sub-canopy layer in a way that avoids the full matrix-exponential calculation in this layer then we can almost halve the overall computational cost. This is only possible if we assume that the sub-canopy layer contains no absorbers or scatterers ($\sigma = \sigma_0 = 0$), i.e. tree trunks and understory vegetation are neglected.

There are two extreme scenarios that lead to $\mathbf{A}_{n-1/2}$ and $\mathbf{D}_{n-1/2}$ having trivial forms. For shrubs with a very shallow sub-canopy layer, the lateral transport between the regions of this layer is zero, leading to albedo matrices at the interface between the canopy and sub-canopy layer being equal to the values at the surface given by (35) and (36). For a very deep sub-canopy layer, the radiation field beneath the canopy is randomized horizontally, leading to the diffuse albedo having the form

$$\mathbf{A}_{n-1/2} \simeq \begin{pmatrix} c^a & c^a & c^a \\ c^b & c^b & c^b \\ c^c & c^c & c^c \end{pmatrix} \overline{\alpha_{\text{diff}}}, \tag{A1}$$

where $\overline{\alpha_{\text{diff}}}$ is the domain-averaged surface albedo to diffuse radiation. The direct albedo $\mathbf{D}_{n-1/2}$ has a similar form.

For sub-canopy layers with a depth between these two extremes, we seek to optimize the calculation of the matrix exponential. The lack of scattering means that the $\mathbf{\Gamma}_2$, $\mathbf{\Gamma}_3$ and $\mathbf{\Gamma}_4$ sub-matrices contain only zeros, and $\mathbf{\Gamma}$ becomes block-diagonal. This enables the exponential of a $3m \times 3m$ matrix to be replaced by three $m \times m$ matrix-exponential calculations, only two of which are needed: $\mathbf{E}_0 = \exp(\mathbf{\Gamma}_0 \Delta z)$ and $\mathbf{E}_{vv} = \exp(\mathbf{\Gamma}_1 \Delta z)$. Since there is no scattering in the sub-canopy layer, the matrices $\mathbf{R}$, $\mathbf{S}^+$ and $\mathbf{S}^-$ contain only zeros. Therefore, (27) simplifies to $\mathbf{T} = \mathbf{E}_{vv}$, and (33) and (34) simplify to

$$\mathbf{A}_{n-1/2} = \mathbf{T}_n \mathbf{A}_{n+1/2} \mathbf{T}_n; \tag{A2}$$

$$\mathbf{D}_{n-1/2} = \mathbf{T}_n \mathbf{D}_{n+1/2} \mathbf{E}_{0n}. \tag{A3}$$

Moreover, by approximating the extinction coefficients as zero, we see from (3) and (4) that $\mathbf{\Gamma}_0$ and $\mathbf{\Gamma}_1$ have simpler forms whose matrix exponentials can be derived analytically. In the $m = 2$ case these matrices have the form

$$\mathbf{\Gamma}' = \begin{pmatrix} -a & b \\ a & -b \end{pmatrix}, \tag{A4}$$

for which the matrix exponential is given by Putzer's algorithm as

$$\exp\left(\mathbf{\Gamma}'\Delta z\right) = \mathbf{I} + \frac{1 - \mathrm{e}^{-(a+b)\Delta z}}{a+b}\mathbf{\Gamma}'. \tag{A5}$$

Likewise in the $m = 3$ case these matrices have the form

$$\mathbf{\Gamma}' = \begin{pmatrix} -a & b & 0 \\ a & -b-c & c \\ 0 & c & -c \end{pmatrix}, \tag{A6}$$

for which the matrix exponential may be computed by the diagonalization method as

$$\exp\left(\mathbf{\Gamma}'\Delta z\right) = \mathbf{V} \begin{pmatrix} \mathrm{e}^{\lambda_1 \Delta z} & & \\ & \mathrm{e}^{\lambda_2 \Delta z} & \\ & & 1 \end{pmatrix} \mathbf{V}^{-1}, \tag{A7}$$

where the two non-zero eigenvalues are

$$\lambda = -(a+b+2c)/2 \pm (a^2 + b^2 + 4c^2 + 2ab - 4ac)^{1/2}/2, \tag{A8}$$

and the matrix of eigenvectors is

$$\mathbf{V} = \begin{pmatrix} b/(a+\lambda_1) & b/(a+\lambda_2) & b/a \\ 1 & 1 & 1 \\ c/(c+\lambda_1) & c/(c+\lambda_2) & 1 \end{pmatrix}. \tag{A9}$$

*Acknowledgements.* We thank Jean-Luc Widlowski for providing the Monte Carlo results. TQ's contribution was funded by the UK National Centre for Earth Observation. RB was supported by a scholarship from the Brazilian 'Science without Borders' Program (grant number 9549-13-7), financed by CAPES, the Brazilian Federal Agency for Support and Evaluation of Graduate Education within the Ministry of Education of Brazil.

## References


Best, M. J., M. Pryor, D. B. Clark, G. G. Rooney, R. L. H. Essery, C. B. Ménard, J. M. Edwards, M. A. Hendry, A. Porson, N. Gedney, L. M. Mercado, S. Sitch, E. Blyth, O. Boucher, P. M. Cox, C. S. B. Grimmond and R. J. Harding, 2011: The Joint UK Land Environment Simulator (JULES), model description. 1: Energy and water fluxes. *Geosci. Model Dev.*, **4,** 677–699.

Hansen, M., R. S. DeFries, J. R. G. Townshend, M. Carroll, C. Dimiceli and R. A. Sohlberg, 2003: Global percent tree cover at a spatial resolution of 500 meters: First results of the MODIS vegetation continuous fields algorithm, *Earth Interact.*, **7,** 1–15.

Higham, N. J., 2005: The scaling and squaring method for the Matrix Exponential revisited. *SIAM J. Matrix Anal. Appl.*, **26,** 1179–1193.

Hogan, R. J., and J. K. P. Shonk, 2013: Incorporating the effects of 3D radiative transfer in the presence of clouds into two-stream multilayer radiation schemes. *J. Atmos. Sci.*, **70,** 708–724.

Hogan, R. J., and A. Bozzo, 2016: ECRAD: A new radiation scheme for the IFS. ECMWF Technical Memorandum 787, 33 pp.

Hogan, R. J., S. A. K. Schäfer, C. Klinger, J.-C. Chiu and B. Mayer, 2016: Representing 3D cloud-radiation effects in two-stream schemes: 2. Matrix formulation and broadband evaluation. *J. Geophys. Res. Atmos.*, **121,** 8583–8599.

Jensen, M. P., A. M. Vogelmann, W. D. Collins, G. J. Zhang and E. P. Luke, 2008: Investigation of regional and seasonal variations in marine boundary layer cloud properties from MODIS observations. *J. Climate,* **21,** 4955–4973.

Lacis, A. A., and J. E. Hansen, 1974: A parameterization for the absorption of solar radiation in the Earth's atmosphere. *J. Atmos. Sci.,* **31,** 118–133.

Loew, A., P. M. van Bodegom, J.-L. Widlowski, J. Otto, T. Quaife, B. Pinty and T. Raddatz, 2014: Do we (need to) care about canopy radiation schemes in DGVMs? Caveats and potential impacts. *Biogeosci.*, **11,** 1873–1897.

Meador, W. E., and W. R. Weaver, 1980: Two-stream approximations to radiative transefer in planetary atmospheres: a unified description of existing methods and a new improvement. *J. Atmos. Sci.,* **37,** 630–643.

Morcrette, C. J., 2012: Improvements to a prognostic cloud scheme through changes to its cloud erosion parametrization. *Atmos. Sci. Lett.*, **13,** 95–102.

Ni-Meister, W., W. Yang and N. Y. Kiang, 2010: A clumped-foliage canopy radiative transfer model for a global dynamic terrestrial ecosystem model. 1: Theory. *Ag. Forest Meteorol.*, **150,** 881–894.

Pinty, B., T. Lavergne, R. E. Dickinson, J.-L. Widlowski, N. Gobron and M. M. Verstraete, 2006: Simplifying the interaction of land surfaces with radiation for relating remote sensing products to climate models, *J. Geophys. Res.*, **111,** doi:10.1029/2005JD005952.

Putz, F. E., G. G. Parker and R. M. Archibald, 1984: Mechanical abrasion and intercrown spacing. *Am. Midland Naturalist,* **112,** 24–28.

Schäfer, S. A. K., R. J. Hogan, C. Klinger and B. Mayer, 2016: Representing 3D cloud-radiation effects in two-stream schemes: 1. Longwave considerations and effective cloud edge length. *J. Atmos. Sci.*, **121,** 8567–8582.

Sellers, P. J., 1985: Canopy reflectance, photosynthesis and transpiration. *Int. J. Remote Sens.*, **6,** 1335–1372.

Shonk, J. K. P., and R. J. Hogan, 2008: Tripleclouds: An efficient method for representing horizontal cloud inhomogeneity in 1D radiation schemes by using three regions at each height. *J. Climate,* **21,** 2352–2370.

Simard, M., N. Pinto, J. B. Fisher and A. Baccini, 2011: Mapping forest canopy height globally with spaceborne lidar. *J. Geophys. Res. Biogeosci.*, **116,** doi:10.1029/2011JG001708.

Tiedtke, M., 1996: An extension of cloud-radiation parameterization in the ECMWF model: the representation of subgrid-scale variations of optical depth. *Mon. Wea. Rev.*, **124,** 745–750.

Viterbo, P., and A. K. Betts, 1999: Impact on ECMWF forecasts of changes to the albedo of the boreal forests in the presence of snow. *J. Geophys. Res.*, **104,** 27803–27810.

Waterman, P. C., 1981: Matrix-exponential description of radiative transfer. *J. Opt. Soc. Am.*, **71,** 410–422.

Widlowski, J.-L., B. Pinty, M. Clerici, Y. Dai, M. De Kauwe, K. de Ridder, A. Kallel, H. Kobayashi, T. Lavergne, W. Ni-Meister, A. Olchev, T. Quaife, S. Wang, W. Yang, Y. Yang and H. Yuan, 2011: RAMI4PILPS: An intercomparison of formulations for the partitioning of solar radiation in land surface models. *J. Geophys. Res. Biogeosci.*, **116,** doi:10.1029/2010JG001511.